CFD Simulation of Internal Flowfield of Dual-mode Scramjet

C. Butcher, K. Yu

Department of Aerospace Engineering, University of Maryland, College Park, MD, USA

Abstract: The internal flowfield of a hypersonic airbreathing engine, as that which is found in a dual-mode scramjet engine, is very complex. The incredibly high temperatures seen in supersonic and hypersonic flows, transverse fuel injection into a supersonic cross-flow and sustaining supersonic combustion are only a couple of the reasons for such complexity. Heat addition downstream of the combustion zone causes a shock train to form upstream of the fuel injection location in order to match the pressure rise associated with said heat release. Properly modeling these phenomena is non-trivial. Several approaches taken by the authors are presented below. The results were found to have good agreement when compared to experimental data that was gathered from a model scramjet in the Hypersonic Center at the University of Maryland, College Park [1].

Keywords: CFD, scramjet, shock train, heat release, transverse fuel injection

1. Introduction

The purpose of this research was to simulate the internal flowfield of a dual-mode scramjet combustor, including shock trains and thermal choking characteristics. The authors also aimed to quantitatively deduce the spatial distribution of heat release characteristics obtained in the experiments by calibrating the wall pressure profiles and boundary conditions.

This paper presents the methods that were taken by the authors. For simplicity and to reduce computational cost, the simulations were split into two separate parts: the isolator and combustor. This allowed each part to be more accurately modeled with greatly reduced computational cost than to model the entire geometry at once. Each model was subjected to a number of different conditions and will be presented below. At each step, the results were compared to experimental data that were gathered from the model scramjet. This was done to validate the simulations and give them a basis for comparison. The results showed good agreement in most cases, even with several simplifications and assumptions that were taken by the authors. The main goal is to develop an approximate technique to extract heat release information from experimentally obtained pressure profile data when optical access or heat release data is unavailable. This will help gain additional insight into the performance and characteristics of the model scramjet.

2. Basic Theory and COMSOL Setup

For all of the simulations that were performed, the fully compressible Navier-Stokes equations govern the fluid flow. These are found in [2] and [3]. The Navier-Stokes equations are a set of 3 individual equations derived using the conservation of mass, momentum, and energy. The conservation of mass, or continuity equation, is as follows:

$$\frac{\partial \rho}{\partial t} + \nabla \cdot (\rho u) = 0 \qquad (1)$$

where bold quantities represent vectors in all equations. Equation 1 states that mass can neither be created nor destroyed: it must remain constant for a given control volume [3]. The second Navier-Stokes equation is derived from the conservation of momentum.

$$\rho \frac{\partial u}{\partial t} + \rho(u \cdot \nabla)u = \nabla \cdot [-pI + \tau] + F \quad (2)$$

Equation 2 states that the time rate of change of momentum must be equivalent to the force exerted on the body [3]. The body force terms are on the right side of the equation. The third and final equation is derived using the conservation of energy.

$$
\begin{aligned}
\rho C_p &\left(\frac{\partial T}{\partial t} + (u \cdot \nabla)T \right) \\
&= -(\nabla \cdot q) + \tau : S \\
&\quad - \frac{T}{\rho} \frac{\partial \rho}{\partial T}\bigg|_p \left(\frac{\partial p}{\partial t} \right. \\
&\quad \left. + (u \cdot \nabla)p \right) + Q
\end{aligned}
\qquad (3)
$$

Where τ is the viscous stress tensor, q is the heat flux vector, and Q is the heat source over a volumetric domain [2]. Equation 3 states that

energy must remain constant. It can change form, but it cannot be created nor destroyed [3].

All of the simulations presented herein were done using COMSOL 4.4 and the turbulent *High Mach Number Flow* branch of the CFD module. The first step in simulating the model scramjet in COMSOL was to generate the geometry. Due to its relatively simple design, a series of basic shapes were used to model the internal flowpath in 2D space. This was done using a rectangle for the isolator and a Bézier polygon consisting of line segments for the combustor and nozzle. The correct material properties were applied for the fluid and the inlet/outlet boundaries were added. For the isolator, the inlet conditions were set as shown in Table 1. The Reynolds number is calculated based on the isolator inlet height and the viscosity can be found in [4].

Table 1. Scramjet Inlet Conditions [1]

Mach Number	2.0419
Static Temperature	699.7 [K]
Static Pressure	83304.2 [Pa]
Total Pressure	683928.9 [Pa]
Reynolds Number	154,119
Fuel Mass Flow Rate	0.377 [g/s]

The isolator outlet was set to a hybrid flow condition with the static pressure equal to the approximate values seen at the zero location in the model scramjet. More information can be found in section 3 below.

For both the isolator and combustor simulations, a series of three stationary studies were run each time in order to accurately model a no slip wall condition. The reasoning for this will be presented in section 3. In each study, the dynamic viscosity was decreased through a set range of values each time, artificially increasing the Reynolds number through the use of an auxiliary sweep. This method was adapted from the *Transonic Flow in a Nozzle* tutorial from COMSOL [5]. The first two *stationary* studies used COMSOL's $k - \epsilon$ turbulence model and utilized a *slip* wall boundary condition and *wall functions*. The third study, a *stationary with initialization* study, used the Spalart-Allmaras turbulence model and the *no slip* wall condition. The second and third studies had the values of the dependent variables initialized using the solution from the previous study and were run through the auxiliary sweep.

3. Isolator Simulation

The purpose of an isolator in a dual-mode scramjet engine is to facilitate a pressure rise caused from the combustion downstream without allowing the engine to unstart. If that were to happen, the flow inside the engine would become purely subsonic, greatly reducing performance or even preventing the engine from being able to operate altogether [7]. The pressure rise is facilitated by the subsonic boundary layer that exists in a flow with a no slip wall. That is where the difficulty of properly modeling the model scramjet arises. The solution procedure can be found in section 2 above. The no slip wall causes boundary layer separation and the formation of a shock train. Shock trains can have an oblique or a normal shock structure as shown in Fig. 1a. An oblique shock train produces a smooth, fairly uniform pressure rise as seen in Fig. 2. However, a normal shock train produces a pressure rise that resembles a stair step fashion and causes a greater loss of stagnation pressure – a key airbreathing engine performance measure. The pressure rise from a normal shock train can be seen in Fig. 3. It is the difference in shock train structures that explains the difference between the pressure rises in Figs. 2 and 3. As will be seen later in Fig. 7b, the model scramjet had an oblique shock train but
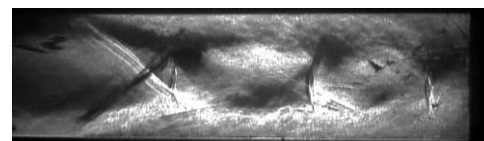
(a) Experimental schlieren photograph visualizing vertical density gradient [6]
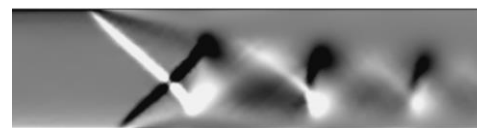
(b) COMSOL simulation showing vertical density gradient in isolator of dual-mode scramjet engine.

Figure 1. Experimental (a) and simulated (b) shock trains in a constant area duct. Black and white indicate a negative and positive density gradient, respectively. Both images show a normal shock train structure.
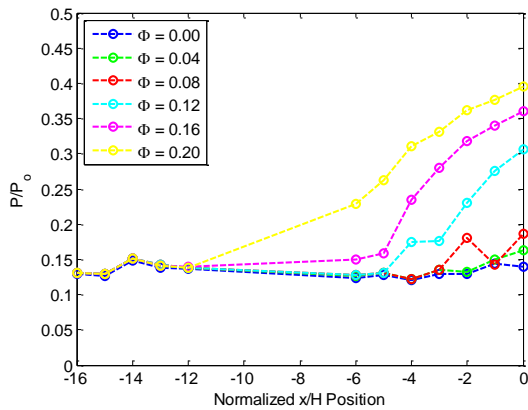
Figure 2. Normalized experimental static pressure measurements along top wall of isolator for all combustor equivalence ratios. Adapted from [1].

the simulations generated a normal shock structure as shown in Figs. 1b and 4.

The isolator is a very simple 0.5" square by 8.5" long duct. There are static pressure ports along the top wall spaced at 0.5" increments. The time averaged data from these measurements was shown in Fig. 2. As expected, the higher the combustor equivalence ratio, Φ, the higher the pressure at the exit of the isolator/entrance to the combustor. As stated before, this is because the pressure increase due to the exothermic reaction forces the flow upstream to adjust. Simulations were run for all combustor equivalence ratios from the experiment. This not only allowed for the generation of the pressure data in Fig. 3, but also allowed for comparison of the shock train structures. This can be seen in Fig. 4. It is
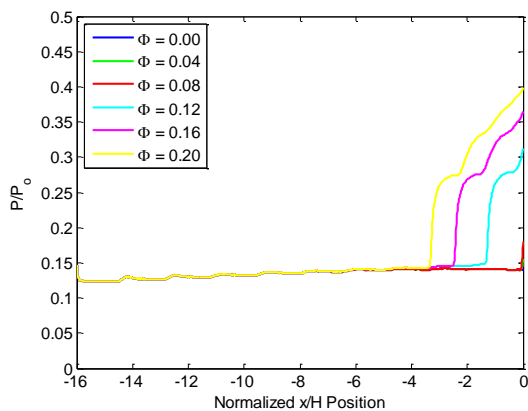

Figure 3. Simulated static pressure measurements along top wall of isolator for all combustor equivalence ratios.

expected that for the cold flow case, $\Phi = 0.00$, there would be no shock structure because there is no pressure rise to account for. This is seen in Fig. 4a. As the back pressure is increased due to the higher combustor equivalence ratio, a shock train forms and propagates upstream. The increasing number of shocks allows for the higher static pressure rise that is needed.

4. Combustor Simulation

Due to the boundary layer and shock train, all of the exit conditions from the isolator have a profile in the vertical direction. Because the geometry was split into two distinct sections, outlet values from the isolator were used as inlet values for the combustor. This caused an issue because some average or constant value had to be chosen for the Mach number, temperature, and pressure rather than the full profile. In order to find the best combination of combustor inlet parameters, a series of cold flow simulations with no heat release or fuel injection were run varying these values within the ranges seen at the exit of the isolator. This is seen in Fig. 5.

In order to select which set of data to use for the input conditions, the area downstream of the combustion zone became the focus. The simulated data needed to closely match the experimental measurements in this area from x/H of 6 onward. Two of the simulated cases became the focus: both of the cases with an inlet pressure of 1.8 atm. The case with the higher temperature and Mach number matches the experimental data most closely, but it is known that adding heat will raise the pressure by a certain amount. If that particular set of values were to have been used, then the downstream pressure would have been too high after the fuel injection and heat addition were added into the model. Therefore, the authors selected the case with 1.8 atm, 950 K, and a Mach number of 1.32 to use for the inlet conditions for all future combustor simulations.

The equivalence ratio of 0.12 was chosen in particular so that the simulations can help gain more insight into the physics of the model scramjet. Due to the difficulties of visualizing an enclosed supersonic flow over such a large length, it is unknown whether or not the flow transitions back to supersonic after it passes through the combustion zone. In order to determine what happens to the flow, there are several parameters that can be explored: determining the actual
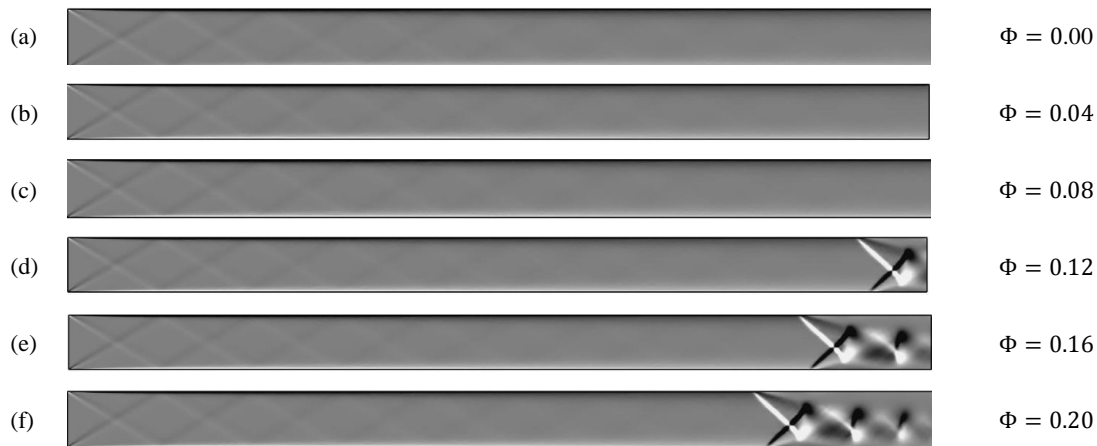
(a)   Φ = 0.00

(b)   Φ = 0.04

(c)   Φ = 0.08

(d)   Φ = 0.12

(e)   Φ = 0.16

(f)   Φ = 0.20

Figure 4. Simulated density gradients for all fuel flow conditions. The data in Fig. 3 was taken from these simulations.

amount of heat that was given off during the experiments and the exact location of that release. The first step was to estimate the amount of heat release that would most likely be seen in the model scramjet. To do this, a heat release value was calculated based on the heat of reaction of the hydrogen fuel – 119,954 kJ/kg fuel [7]. Due to the effects of dissociation seen in high temperature gas dynamics and material properties limitations, an upper limit of 3,000 K was imposed. This limits the fuel to about one third of the maximum heat that could be released in an ideal stoichiometric reaction. That translates to a total power for the heat release of about 950 kW per unit width over the heat release domain. Based on

Figure 5. Normalized simulated static pressure measurements along top wall of combustor as a function of combustor inlet conditions. Simulations were for cold flow with no fuel injection. Experimental data from [1].

these assumptions and properties, a range of simulations were run at or below this value. The results are shown in Fig. 6.

As predicted before, the larger the amount of heat that is released, the higher the downstream pressure values. However, the simulation with 1/6 of the lower heating value of hydrogen fuel shows very good agreement downstream. In addition, it oscillates about the experimental values in the area above the cavity. The discrepancy is to be expected because of several issues that are discussed in section 5 below.

5. Issues

It is difficult to compare these simulations number for number with the model scramjet. The geometry cross section is the same, but the simulations were completed in 2D – a far cry from the 3D experiments. While COMSOL was able to generate the shock trains in the isolator, they are an inherently three dimensional, asymmetric structure in real life. The boundary layer would be on all four walls of the scramjet, whereas the simulations only have a boundary layer on the top and bottom surfaces. Another issue is that the model scramjet would have had a large amount of heat transfer into the stainless steel walls, especially during the first few seconds of each run while they warm up from room temperature. Last but not least, the experimental measurements are time averaged over runs of up to ten seconds. The COMSOL simulations are stationary solutions at one instant in time. This explains why the curves in Fig. 6 oscillate about the experimental value.
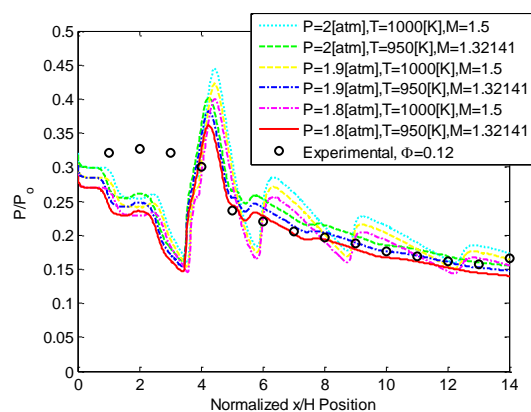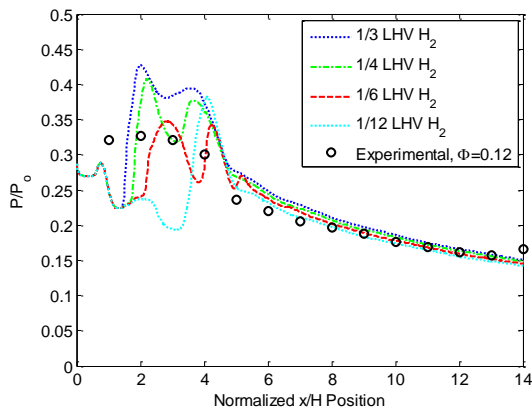
Figure 6. Normalized simulated static pressure along top wall of combustor as a function of combustor equivalence ratio. Experimental data from [1].

As the flame fluctuates in the cavity, the pressure will fluctuate as well. Time averaging the data evens out those oscillations and make it appear as a nice smooth curve. In order to compare results with the model scramjet, they must oscillate about one another and follow the same general trends.

6. Conclusions

The model scramjet was simulated in two distinct sections: the isolator and combustor. This aided with convergence, greatly reduced time and computational cost, and was able to better generate flow features as seen in the model scramjet. All simulations were run in 2D with the turbulent *High Mach Number Flow* branch of the CFD module in COMSOL Multiphysics 4.4. Using a set of three studies, each simulation was run through a *slip, wall functions,* and *no slip* wall boundary condition. This aided in convergence and ensured that all simulations were subjected to the same process. The *no slip* wall condition allowed for the creation of a shock train in the isolator. Each combustor equivalence ratio generates a different pressure rise, all of which were able to be matched through the simulations. There were some discrepancies however, as COMSOL generated normal shock train structures, whereas an oblique structure was seen in the experiments [1].

The isolator exit conditions were applied to the combustor inlet and the simulations were run through several sets of boundary conditions in order to best match the experimental measurements downstream. This was due to difficulties in implementing the full exit profiles. Once a reasonable set of conditions were found, the fuel injection and heat addition were added into the model. A range of heat release values were applied over the same domain area in order to find an estimated amount of heat that was released in the model scramjet. It was found that the authors' assumptions were correct in that the heat release was found to be less than the upper limit that was proposed.

7. Future Work

Now that a basic scramjet model has been set up, the heat release can be tweaked to more closely match the experimental data. In order to do this, the heat release domain can be altered in shape or size, as well as intensity in order to gain additional insight into the combustion zone of the model scramjet. Another method will be to use a series of several smaller domains with differing heat release values rather than a single domain at one constant intensity. Once this is completed, focus can shift to modeling the model scramjet with the added fin upstream of the fuel injection location. The fin allows for better fuel penetration into the cross-flow and allows the combustion to take place further downstream. It is thought that this prevents the dual-mode scramjet from becoming thermally choked as is possible in the baseline case. This can be seen in Fig. 7. The change in shock structures can also be seen. In Fig. 7b there is an oblique shock train in the isolator and beginning of the combustor, whereas the fin case (Fig. 7c) has a much more simple shock structure originating mostly from the fin and fuel injection. It is these types of structures that hope to be modeled in the future.

8. References

[1] Muñoz, Camilo A., Effect of Fin-Guided Fuel Injection on Supersonic Mixing and Combustion, PhD Dissertation, University of Maryland, College Park (2014).

[2] COMSOL, CFD Module User's Guide, CFD Module Documentation (2013).

[3] Anderson, John D., *Modern Compressible Flow with Historical Perspective*, pp. 239-260. McGraw Hill, New York (2003).
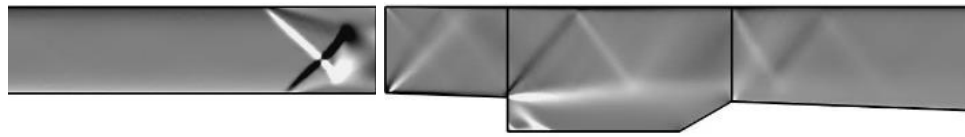
(a) COMSOL simulation for baseline reacting case with $\Phi = 0.12$ showing vertical density gradient in isolator *(left)* and combustor *(right)*. The gap represents that the simulations were run separately and is equivalent to 0 location in (b) and (c) below. The vertical lines in the right portion of the image represent the left and rightmost bundaries of the heat release domain. Far upstream and downstream have been cut off in this illustration.
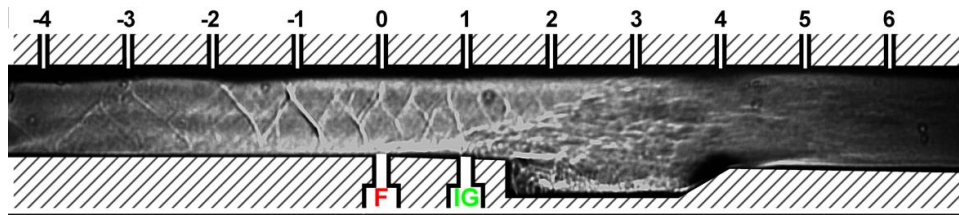
(b) Experimental schlieren image for baseline case and $\Phi = 0.12$. The combustion zone can be seen in the cavity between locations 1 and 4 [1].
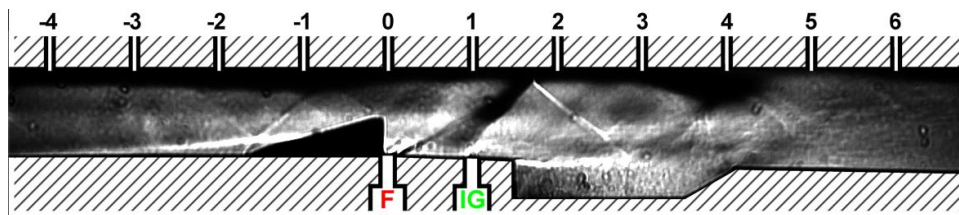
(c) Experimental schlieren image for fin case and $\Phi = 0.12$. Due to the addition of the 3-D fin upstream of the cavity, most of the combustion takes place in the diverging area downstream of the combustor. [1].

Figure 7. Simulated and experimental schlieren images for baseline (a,b) and fin case (c). In (b) and (c), the 'F' and 'IG' represent the fuel and igniter locations, respectively.

[4] Kadoya, K., Matsunaga, N., and Nagashima, A, Viscosity and Thermal Conductivity of Dry Air in the Gaseous Phase, *J. Phys. Chem. Ref. Data*, **Vol. 14, No. 4**, pp. 947-970 (1985).

[5] COMSOL, Transonic Flow in a Nozzle, COMSOL Model Library Tutorial (2012).

[6] Geerts, Jonathan, PhD Candidate at University of Maryland, College Park (2014).

[7] Heiser, William H. and Pratt, David T., *Hypersonic Airbreathing Propulsion*, pp. 113,251-257. American Institute of Aeronautics and Astronautics, Washington, DC (1994).

9. Acknowledgments